Journal of Applied Polymer Science

Influence of Polymeric Flame Retardants Based on Phosphorus-Containing Polyesters on Morphology and Material Characteristics of Poly(butylene terephthalate)

Thomas Köppl,[1] Sven Brehme,[2] Doris Pospiech,[3] Oliver Fischer,[3] Felipe Wolff-Fabris,[1] Volker Altstädt,[1] Bernhard Schartel,[2] Manfred Döring[4]

[1]University of Bayreuth, Department of Polymer Engineering, Bayreuth 95447, Germany
[2]BAM Federal Institute for Materials Research and Testing, Berlin 12205, Germany
[3]Leibniz Institute of Polymer Research Dresden, Dresden 01069, Germany
[4]Deutsches Kunststoff-Institut, Darmstadt 64289, Germany
Correspondence to: T. Köppl (E-mail: thomas.koeppl@uni-bayreuth.de)

ABSTRACT: Flame retarded poly(butylene terephthalate) (PBT) is required for electronic applications and is mostly achieved by low molar mass additives so far. Three phosphorus-containing polyesters are suggested as halogen-free and polymeric flame retardants for PBT. Flame retardancy was achieved according to cone calorimeter experiments showing that the peak heat release rate and total heat evolved were reduced because of flame inhibition and condensed-phase activity. The presented polymers containing derivatives of 9,10-dihydro-9-oxa-10-phosphaphenanthrene-10-oxide form immiscible blend systems with PBT. Shear-rheology shows an increase in storage moduli at low frequencies. This is proposed as quantitative measure for the degree of phase interaction. The phase structure of the blends depends on the chemical structure of the phosphorus polyester and was quite different, depending also on the viscosity ratio between matrix and second phase. A lower viscosity ratio leads to two types of phases with spherical and additionally continuous droplets. Addition of the flame retardants showed no influence on the dielectric properties but on the mechanical behavior. The polymeric flame retardants significantly diminish the impact strength because of several reasons: (1) high brittleness of the phosphorus polyesters themselves, (2) thermodynamic immiscibility, and (3) weak phase adhesion. By adding a copolymer consisting of the two base polymers to the blend, an improvement of impact strength was obtained. The copolymer particularly acts as compatibilizer between the phases and therefore leads to a smaller phase size and to a stronger phase adhesion due to the formation of fibrils.
© 2012 Wiley Periodicals, Inc. J. Appl. Polym. Sci. 000: 000–000, 2012

KEYWORDS: polyesters; blends; miscibility; rheology; flame retardance

Received 20 June 2012; accepted 28 August 2012; published online
DOI: 10.1002/app.38520

INTRODUCTION

As most standard and technical thermoplastics are easily flammable, they categorically need flame and fire protection for technical usages. Poly(butylene terephthalate) (PBT) is a technical thermoplastic material that is mainly used in electrical and electronic applications where adequate mechanical strength, electrical isolation, and flame retardancy play a decisive role. Halogen-free flame retardancy of polymers is gaining more and more attention due to the aim of avoiding chlorine- and bromine-based flame retardants.[1,2] Such halogen-containing additives are very efficient but form very toxic substances like halogenated hydrocarbons, dioxins, and furans in case of fire. Also relevant for electrical and electronic applications is the problem that some halogen-containing flame retardants can cause corrosion on the metallic contact area due to blooming of the flame retardant.[3] Today, the flame retardancy of PBT is still predominantly achieved by halogen-containing substances like bromo polystyrene, tetrabromo bisphenol A polycarbonate, and decabromo diphenyl oxide.[3] An alternative to halogenated flame retardants consists in phosphorus compounds that act both in the gas phase and in the condensed phase.[4–6] Unfortunately, the necessary amount of halogen-free additives is usually significantly higher than that of halogen derivatives. Some of the few halogen-free flame retardants for PBT that are already commercially available are additives based on metal phosphinates like aluminum and zinc phosphinates.[7,8] The main drawback of these low-molar mass additives is the mechanical deterioration of the polymer matrix. A new approach that might overcome

© 2012 Wiley Periodicals, Inc.

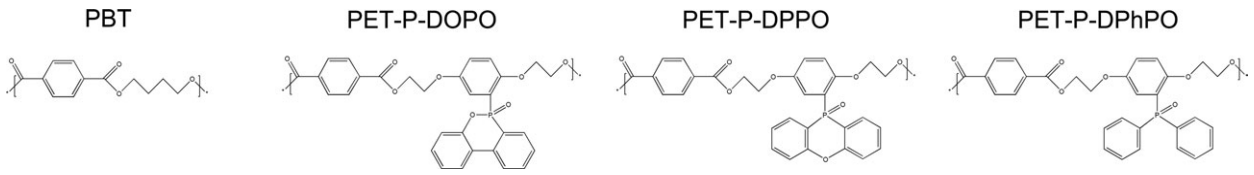

Figure 1. Chemical structures of PBT and the synthesized polymers PET-P-DOPO, PET-P-DPPO and PET-P-DPhPO.

the above-mentioned problems is the preparation of flame retardants with a polymer backbone. In contrast to low-molar mass flame retardants, polymeric ones are chemically bound to the polymer and can therefore lead to a better mechanical performance of the polymer, because no fillers are required, which act as matrix imperfections. In previous works, polyesters containing the flame-retarding substance 9,10-dihydro-9-oxa-10-phosphaphenanthrene-10-oxide (DOPO) have been successfully synthesized.[9,10] In recent studies, it was shown that DOPO-containing polyesters[11,12] and copolymers with PBT[13] were used as effective additives in PBT but resulted in immiscible blend systems. The comparison of the efficiency of one of the phosphorus polyesters with low-molar mass flame retardants for PBT has recently been published.[6,14]

In this work, new phosphorus polyesters were applied as flame retardants for PBT and compared regarding morphology and miscibility of the flame retardants with PBT. These structural results were correlated to the material characteristics. The influence of the phase structure on processability, dielectric properties, mechanical performance, and flame retardance is investigated. To improve the miscibility of the polymer phases, copolymers of PBT and one of the phosphorus polyesters were synthesized as compatibilizers and were also investigated here.

EXPERIMENTAL

Flame Retardant (Phosphorus Polyester) Synthesis

Three polymeric halogen-free phosphorus-containing polymers were synthesized by melt transesterification polycondensation from dimethyl terephthalate and different phosphorus containing diols. The syntheses and results (molar masses) were already reported elsewhere.[10–12] The resulting polymers are phosphorus-containing polyesters, abbreviated as PET-P-x (Polyethylene terephthalate, x: abbreviation of substituent name), with varying chemical structure of the phosphorus-containing substituent. The chemical structures of PBT and the phosphorus polymers PET-P-DOPO, PET-P-DPPO, and PET-P-DPhPO are presented in Figure 1.

Besides, the phosphorus homopolyesters also a random copolymer of PBT and PET-P-DOPO (in 50 : 50 mol : mol ratio) referred to as PBT-*co*-PET-P-DOPO was synthesized and characterized as described previously[12,13] for application as compatibilizer between PBT an d PET-P-DOPO in their blend.

Processing of Compounds

An injection-molding grade of PBT (Ultradur B4520, BASF SE, Ludwigshafen, Germany) was melt compounded at 250°C using a corotating twin-screw extruder (Brabender DSE 20/40, Duisburg, Germany) with length-to-diameter ratio of 40 and screw diameter of 20 mm. The dried polymeric flame retardants were supplied in the main feeder together with the dried PBT. The compounded material was again dried for at least 4 h at 80°C. The test samples were produced by injection molding on a Krauss Maffei KM 65/180/55 CX V (Munich, Germany) injection molding machine with a melt temperature of 250°C and a mold temperature of 70°C. The rheological samples were pressed from granules at 250°C in a hot press under vacuum for 5 min and a pressure of 20 kN. The polymeric flame retardants have a lower softening range than PBT and were therefore pressed at 180°C. All specimens were dried at 80°C in a vacuum dryer for at least 24 h before characterization.

Morphology

The blend morphology was characterized by scanning electron microscopy (SEM) on a Zeiss Ultra plus FE-SEM (Oberkochen, Germany) with field emission cathode using an acceleration voltage of 2 kV, after sputter-coating the samples with a thin gold layer. The images were recorded on the fracture surfaces resulting from impact testing of the injection-molded samples. As the materials showed brittle fracture, we assume no deformation of polymer blend phases after impact testing.

Rheological Behavior

The rheological properties of the neat polymers and compounds were analyzed by a stress-controlled dynamic-mechanical rheometer SR 5000 from Rheometric Scientific (TA Instruments, New Castle, Delaware) with plate–plate geometry under nitrogen atmosphere. The samples had a diameter of 25 mm and a height of 2 mm and were analyzed isothermally at 240°C. In dependence of the angular frequency, dynamic-mechanical tests were performed to compare the complex viscosity and moduli of the materials. Each measurement was repeated at least four times. Before measuring frequency-dependent values like complex viscosity and storage modulus, the optimal stress for measuring in linear regime was determined by stress-sweep measurements. To be sure that no degradation and cross-linking processes take place, time-sweep measurements were performed to obtain the stability time of the polymers for measurements excluding molecular effects.

Thermal Analysis

The thermal behavior of the polymers was investigated by differential scanning calorimetry (DSC). Standard DSC measurements were done with a Mettler Toledo (Columbus, Ohio) DSC/SDTA 821 e under nitrogen atmosphere with a heating and cooling rate of 10 K/min. The crystallinity was analyzed with an enthalpy of fusion of 100% crystalline PBT of 140 J/g[15] and normalized to the amount of PBT in the blend.

Modulated DSC measurements were carried out in the range of 23–260°C at a scan rate of 2 K/min with amplitude of ±0.31 K and a period of 40 s on a DSC Q1000 from TA Instruments in nitrogen atmosphere (flow rate 50 mL/min). From these

Table I. Composition and Crystallinity of the Processed Compounds

Material	Composition (wt %)	Crystallinity of PBT portion (%)
PBT	100/0	33 ± 1
PBT/PET-P-DOPO	74/26	34 ± 1
PBT/PET-P-DPPO	73/27	41 ± 1
PBT/PET-P-DPhPO	75/25	39 ± 1
PBT/PET-P-DOPO/ PBT-*co*-PET-P-DOPO	(74/26)/5	37 ± 1

measurements, the glass transition temperatures (T_g) were calculated from the reversing heat flow signal in the second heating run using the half step method. Each measurement was repeated at least three times with a resulting error of 1 K.

The miscibility was also investigated by Dynamic Mechanical Analysis (DMA) with a RDA III Rheometric Scientific (TA Instruments). The samples were taken from injection molded CAMPUS tensile bars (50 × 10 × 4 mm^3). Injection molding was only possible with the blends and not with the brittle PET-P polymers. The miscibility of the blends was analyzed by detecting the glass transitions. Oscillatory measurements starting from room temperature to 180°C were done with a heating rate of 2 K/min, a deformation of 0.05%, and a frequency of 1 Hz. Each measurement was repeated at least three times.

Dielectric Properties

The dielectric properties like the relative permittivity (ε) and dissipation factor (tan δ) were recorded at room temperature by an Agilent E4991A RF Impedance/Material Analyzer (Santa Clara, California) according to DIN 53483. Each material was tested at least four times in the two-parallel-plate mode at 1 GHz. The source was an alternating voltage of 100 mV. The samples were taken from CAMPUS tensile bars (20 × 20 × 4 mm^3).

Mechanical Testing

Static tensile tests were done at room temperature by means of a universal testing machine Zwick Z020 (Ulm, Germany) according to ISO 527 with a cross-head speed of 5 mm/min for determination of Young's modulus E, tensile strength σ_m, and elongation at break ε_m. The CAMPUS tensile bars were injection molded according to ISO 3167 (Type A).

Short-time dynamic unnotched Charpy tests (ISO 179 fU) were performed on an instrumented Zwick/Roell RKP 5113 (Ulm, Germany) with a pendulum energy of 50 J for evaluating the unnotched Charpy impact strength a_{cu} at room temperature. The unnotched samples were again taken from CAMPUS tensile bars (80 × 10 × 4 mm^3).

Flammability Testing

UL 94 according to IEC 60698-11-10 and limiting oxygen index (LOI) according to ISO 4589 were used to assess the flammability (reaction to a small flame) of the materials.

A cone calorimeter (Fire Testing Technology, East Grinstead, UK) according to ISO 5660 was used to assess the fire behavior under forced-flaming combustion. Plate-shaped specimen (100 × 100 × 3 mm^3) were placed in aluminum trays and exposed to an irradiation of 50 kWm^{-2}. Every material was tested at least twice.

RESULTS AND DISCUSSION

The phosphorus polyester additives were added in different concentrations to PBT to achieve a comparable phosphor concentration of 1.5 wt % in the compounds and blends. A phosphorus concentration of 1.5 wt % is expected to be the minimum concentration for effective flame retardancy. The resulting phosphorus polyester amount of 25–27 wt % is rather huge. Thus, a distinct influence of thermodynamic miscibility on the resulting morphology was expected. The compositions of the processed compounds are listed in Table I, which also shows the crystallinity of the specimens. These results will be discussed later.

Morphology

As the morphology of a blend is known to have a significant impact on several material properties, the morphology of the blends prepared here was first evaluated by SEM. The distribution of flame retardants[16] and the morphology[17–19] of the resulting material are important for the flame-retardancy performance. By all means, the miscibility has an influence on the rheological[20] and mechanical[21] properties of the blend.

As illustrated by SEM pictures, the three investigated PBT/PET-P blend systems form immiscible blends with PBT as matrix and PET-P as dispersed phases. A poor connection between the PBT and PET-P phases can be observed in all systems, visible in SEM pictures showing gaps between the phases and sharp phase boundaries (Figures 2–4).

The blend PBT/PET-P-DOPO (Figure 2) shows spherical PET-P-DOPO droplets with a mean diameter of about 1 μm. The droplets are well dispersed in the PBT matrix. The system PBT/PET-P-DPPO (Figure 3) displays a different phase structure. The two phases are also separated, but the PET-P-DPPO phase forms apart from spherical droplets additionally a continuous phase with a rod-like structure (about 2 μm in average). The mean diameter of the spherical PET-P-DPPO phases (200 nm

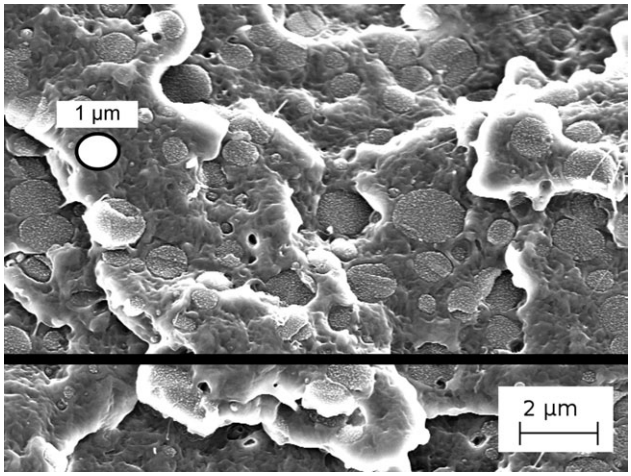

Figure 2. SEM picture of fracture surface after impact testing of PBT/PET-P-DOPO. Magnification: 5000×. One droplet is exemplary highlighted with the average droplet size of 1 μm.

Applied Polymer SCIENCE

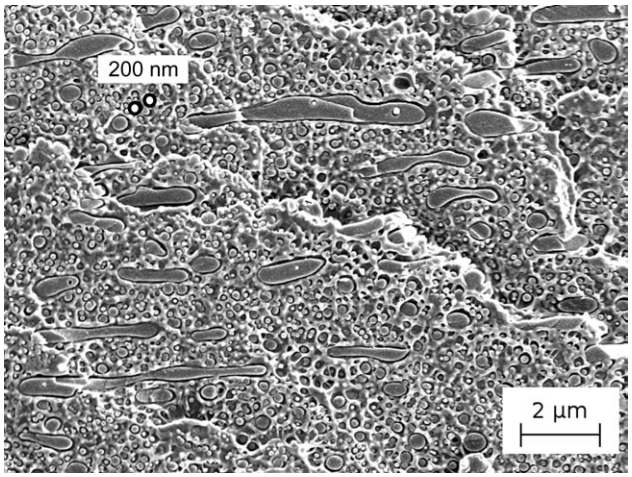

Figure 3. SEM picture of fracture surface after impact testing of PBT/PET-P-DPPO. Magnification: 5000×. Two droplets are exemplary highlighted with the average droplet size of 200 nm.

in average) is significantly smaller and the number of phases is higher than in the above-mentioned blend with PET-P-DOPO phases. The third blend PBT/PET-P-DPhPO is also phase separated (Figure 4) and shows as in the case of PBT/PET-P-DPPO both spherical and continuous phases of PET-P. The spherical phases have a mean diameter of 300 nm, and the continuous phases are longer than in the PBT/PET-P-DPPO system with a length of at least 50 µm. The number of phases is again higher than in the blend PBT/PET-P-DOPO.

It can be expected from the immiscibility of all investigated blends that there is no change in the degree of crystallinity of the PBT portion. Nevertheless, a change in the crystallinity occurs and can be explained by different phase morphologies. The PET-P polymers are amorphous due to the bulky aromatic substituents. Blending with these amorphous polymers enhances the crystallinity of the PBT portion up to 20%. This behavior can be explained by a huge amount of small droplets, especially

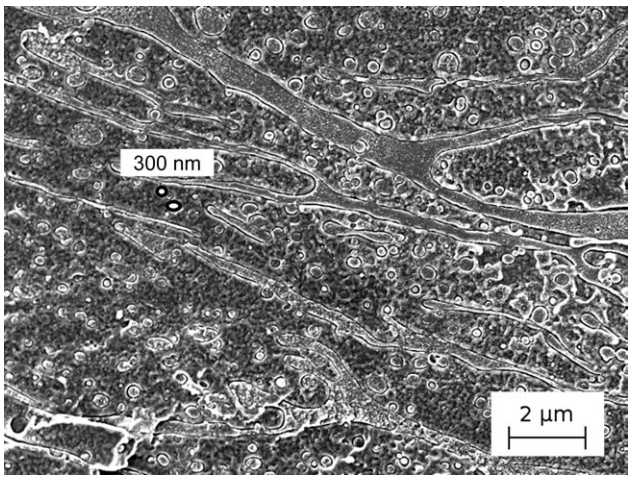

Figure 4. SEM picture of fracture surface after impact testing of PBT/PET-P-DPhPO. Magnification: 5000×. Two droplets are exemplary highlighted with the average droplet size of 300 nm.

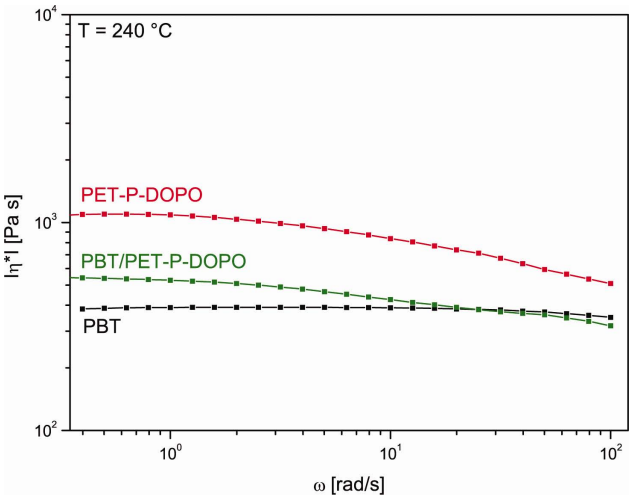

Figure 5. Complex viscosity of PBT/PET-P-DOPO and the base polymers in dependence of the angular frequency obtained by rotational rheometry at 240°C. [Color figure can be viewed in the online issue, which is available at wileyonlinelibrary.com.]

in the systems PBT/PET-P-DPPO and PBT/PET-P-DPhPO, which can act as nuclei for heterogeneous crystallization (see Table I).

Rheological Behavior and Processability

The rheological properties and processability were investigated by means of rotational rheometry. The complex viscosity $|\eta^*|(\omega)$ of the blend systems was determined in dependence of the angular frequency ω and compared to the viscosity of PBT and the corresponding PET-P polymers. In Figure 5, the viscosity of the PBT/PET-P-DOPO system is presented in dependence of the angular frequency.

The viscosity of PET-P shows shear thinning behavior, and the zero shear viscosity is three times higher than that of PBT with Newtonian behavior at all frequencies. Mixing of both polymers results in a zero shear viscosity between the viscosities of the single phases, which means that the viscosity at low frequencies is increased in comparison to PBT. At higher frequencies (>10 s^{-1}), the blend viscosity decreased to the level of PBT.

The other two blend systems showed equal characteristics of their viscosity curves. All blend viscosities obtained are compared to PBT in Figure 6.

At low frequencies, an increase of the blend viscosity is visible, however, no difference is observed at higher frequencies. The decrease of viscosity at high frequencies enables a similar processing of the blends as the neat PBT, as processing usually takes place at frequencies or shear rates, respectively, >100 s^{-1}. The differences between the systems lie in particular in the viscosities of the neat PET-P polymers. The zero shear viscosities of PBT and PET-P polyesters are summarized in Table II.

Although the zero shear viscosities of the PET-P polymers differ in three orders of magnitude, which is mainly due to their different molar masses,[11] the blends, however, show almost the same zero shear viscosity of about 600 Pas (see Figure 6). The

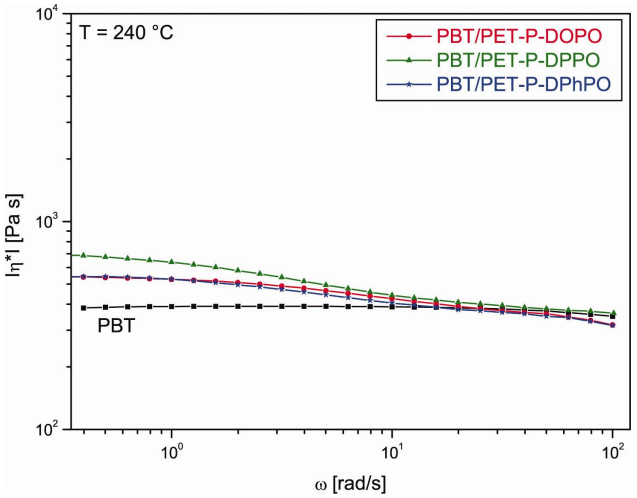

Figure 6. Comparison of the blend viscosities in dependence of the angular frequency: PBT (quadrate), PBT/PET-P-DOPO (circle), PBT/PET-P-DPPO (triangle), and PBT/PET-P-DPhPO (star) obtained by rotational rheometry at 240°C. [Color figure can be viewed in the online issue, which is available at wileyonlinelibrary.com.]

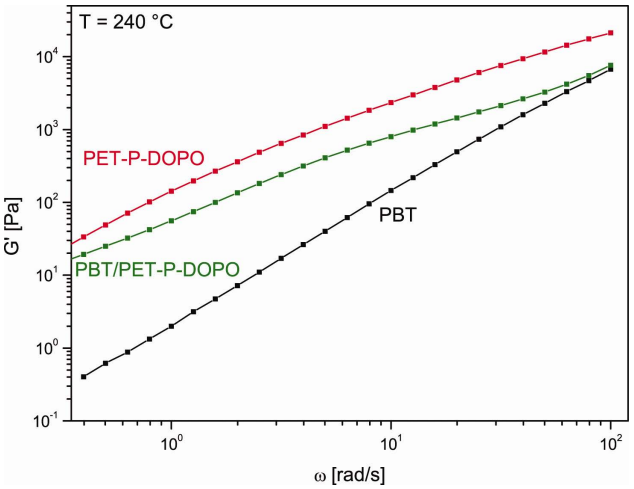

Figure 7. Storage moduli of PBT/PET-P-DOPO and the base polymers in dependence of the angular frequency obtained by rotational rheometry at 240°C. [Color figure can be viewed in the online issue, which is available at wileyonlinelibrary.com.]

difference is reflected by the zero viscosity ratio p, which is defined as

$$p = \frac{\eta_{0,d}}{\eta_{0,m}}$$

where $\eta_{0,d}$ presents the dispersed phase zero viscosity (PET-P) and $\eta_{0,m}$ the matrix zero shear viscosity (PBT). The ratio between the viscosities of the dispersed phases and the matrix differs by three decades in the different systems. The different phase structures can be understood by means of this viscosity ratio and the capillary number Ca, which will be considered later.

The storage modulus G' is a measure for the elasticity of the melt under the given conditions and can be measured by a frequency sweep. The curves obtained for PBT, PET-P-DOPO, and the resulting blend are shown in Figure 7.

PBT shows a linear viscoelastic course of G' over the complete measured frequency range with G' increasing with frequency. Also as observed at the complex viscosity, the storage moduli of the blend at high frequencies approach the value of G' for neat PBT.

This behavior can also be seen in the other two systems. In Figure 8, the storage moduli of all systems are compared to PBT in dependence of the frequency.

Table II. Zero Viscosities and Calculated Zero Viscosity Ratios of PBT and PET-P Polymers Obtained by Rotational Rheometry at 240°C

Material	Zero viscosity η_0 (Pa s)	Zero viscosity ratio p
PBT	400 ± 50	-
PET-P-DOPO	1100 ± 50	2.8
PET-P-DPPO	100 ± 10	0.3
PET-P-DPhPO	10 ± 5	0.03

The shoulder of G' at lower frequencies and the alignment of G' to the storage modulus of PBT can also be seen in PBT/PET-P-DPPO and PBT/PET-P-DPhPO blends. The shoulder of G' in the blend systems at lower frequencies can be explained by an elastic response of the droplet phases as will be discussed later.

Glass Transition Temperatures

As the determination of the glass transition temperatures T_g and the shift in a corresponding blend is a quantitative method for the investigation of miscibility, the glass transition temperatures were measured by DMA as well as by DSC. Although a superimposition of T_g values of these two methods cannot be expected due to the different heating rates used, the immiscibility of all blend systems can be seen by means of DMA

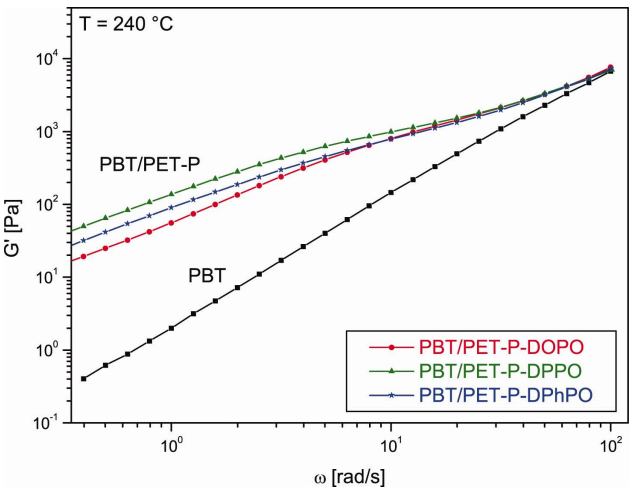

Figure 8. Storage moduli of all blends in dependence of the angular frequency: PBT (quadrate), PBT/PET-P-DOPO (circle), PBT/PET-P-DPPO (triangle), and PBT/PET-P-DPhPO (star) obtained by rotational rheometry at 240°C. [Color figure can be viewed in the online issue, which is available at wileyonlinelibrary.com.]

Applied Polymer SCIENCE

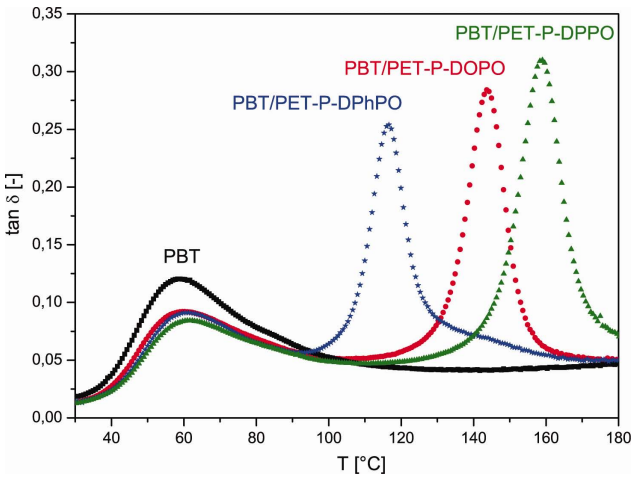

Figure 9. Loss tangent of PBT (quadrate) and the blend systems PBT/PET-P-DOPO (circle), PBT/PET-P-DPPO (triangle), and PBT/PET-P-DPhPO (star) in dependence of the temperature: Maxima of loss tangent represent the glass transitions. [Color figure can be viewed in the online issue, which is available at wileyonlinelibrary.com.]

measurements (Figure 9) detecting two discrete maxima of loss tangent tan δ in each blend. One T_g is located close to the T_g of PBT, and the other glass transition appears at higher temperatures.

With the method of modulated DSC, the glass transition temperature of all materials could be determined in a quantitative way. Table III shows the T_g values of the neat materials and the resulting blends. The results of glass transition temperature will be discussed in the next part regarding the miscibility.

Discussion of Miscibility and Morphology

The appearance of a single T_g in a blend system is an indication of thermodynamic miscibility of the two polymers. If two discrete glass transitions exist, the system is immiscible. By comparison of the glass transitions with the T_gs of the base polymers as well as their respective concentration in the blend, a prediction about the state of demixing can be drawn. Obtaining two glass transitions positioned exactly at the T_gs of the base polymers allows to conclude that the blend is immiscible. A shift of the T_gs toward each other indicates partial compatibility with phase interactions.

As there are two glass transition temperatures in all analyzed blend systems, immiscibility of all blends can be stated (see Table III). In detail, the first T_g is not shifted in any of the systems. The second one is reduced in PBT/PET-P-DOPO and PBT/PET-P-DPhPO compared to the neat PET-P polyesters. These small shifts of T_g point out that there is a partial mixing of the PBT phase into the PET-P-phase, whereas PET-Ps do not diffuse into the PBT phase.[12]

In contrast, the second T_g in the PBT/PET-P-DPPO blend is shifted by about 12 K, that is, interactions between the phases can be assumed. The shift of the second T_g results in partial compatibility of the system PBT/PET-P-DPPO.

The difference in the blend morphologies cannot be correlated to the shift of T_gs but to the different rheological properties of the base polymers and the blends. The currently used approaches to explain the phase deformations are mostly based on the theory of Taylor.[22] He considered the deformation and break-up of Newtonian fluids. To explain the phenomena between the phases, the capillary model is used. The phase structure is described by means of the so-called capillary number Ca and the above-mentioned viscosity ratio p. The capillary number in shear deformation is defined as

$$\mathrm{Ca} = \frac{\eta_m \dot{\gamma}}{\Gamma}$$

where $\dot{\gamma}$ is the shear rate, R is the radius of the drop in a quiescent state, and Γ is the interfacial tension. The course of the critical capillary number in dependence of the viscosity ratio has been considered for non-Newtonian polymer blends in many theoretical and experimental works.[23–26] If the capillary number exceeds a critical value (Ca_{crit}), the drop becomes unstable. In dependence of the viscosity ratio, a drop break-up is assumed.[24]

To describe the morphology of the investigated blends, we have to consider the characteristic values of both Ca_{crit} and p. As we have no information about the interfacial tension Γ, the absolute values of the capillary number cannot be calculated. We assume the location of the capillary number above Ca_{crit} in all blend systems, where drop break-up can occur. Due to the chemical similarity of the base polymers and a similar weak phase connection, we assume also similar values of Ca_{crit}. The viscosity ratio can easily be calculated from base polymer viscosities and therefore will be used for the description of the phase structures.

As the viscosity ratio p is lower than 4 in all investigated blend systems, the breakup of the PET-P phases in the PBT matrix is in principle possible.[23] The lower the viscosity ratio, the more the phases stretch into slender fibrils. The blend PBT/PET-P-DOPO shows, as described earlier, spherical droplets in micrometer scale, which are well dispersed and very regular. The lower viscosity ratio of PBT/PET-P-DPPO results in spherical droplets as well as fibrils. At this viscosity ratio, the drops take a fibrous shape with small droplets releasing from the end (tip

Table III. Glass Transition Temperatures of the Blends and the Base Polymers Obtained by Modulated DSC from the Reversing Heat Flow Signal

Material	T_{g1} (°C; ±1)	T_{G2} (°C; ±1)
PBT	61	-
PET-P-DOPO	-	146
PBT/PET-P-DOPO	60	144
PET-P-DPPO	-	159
PBT/PET-P-DPPO	60	147
PET-P-DPhPO	-	114
PBT/PET-P-DPhPO	60	111

Table IV. Dielectric Permittivity ε and Dissipation Factor tan δ of PBT and the Resulting Blends Obtained in Two-Parallel-Plate Mode

Material	ε	tan δ (10^{-4})
PBT	3.25 ± 0.05	50 ± 3
PBT/PET-P-DOPO	3.34 ± 0.04	60 ± 3
PBT/PET-P-DPPO	3.31 ± 0.02	60 ± 4
PBT/PET-P-DPhPO	3.33 ± 0.02	60 ± 3

streaming),[27] which is the reason for many additional spherical phases at nanometer scale. The blend PBT/PET-P-DPhPO appears also with small spherical droplets and fibrils. The fibrils are significantly more pronounced and form a sigmoidal shape. This can be explained by an even lower viscosity ratio.

The size of the phases and the shift of glass transition temperatures can be linked by considering the elastic properties in the melt. The storage moduli G' of immiscible liquids typically show an enhanced elastic response at low frequencies compared to the matrix moduli.[28] The increase of moduli arises from relaxing of the deformed droplets to a spherical shape. This relaxation depends on the relaxation time and the interfacial tension.

The elastic behavior can be seen at lower frequencies in all investigated blends (Figure 8). We assume that the level of elasticity (G') depends on the type of miscibility, the size of phases, and therefore on the interfacial tension. The higher the interactions between the matrix and the phases the higher is the elastic response.

The blend PBT/PET-P-DPPO exhibits the highest value of G', which is related to the largest glass transition shift (12 K) and therefore to higher interactions than in the other blends. A phase size in nanometer scale reflects larger interactions.

The blend PBT/PET-P-DPhPO shows a small T_g-shift and larger phases of PET-P-DPhPO, resulting in a lower G' than in the blend PBT/PET-P-DPPO. The storage moduli increase of PBT/PET-P-DOPO is even smaller than in the other blends, which is also consistent to almost no T_g-shift and phases with a size of 1 μm.

Dielectric Characteristics

As PBT is often used in electrical housing applications, the insulating properties of the compounds are important. The relative permittivity ε and dissipation factor tan δ should be as low as possible. Hence, the influence of the flame retardants on the dielectric properties is considered, and the results are given in Table IV.

By adding the phosphorus polymers to PBT, there is a small increase of ε and tan δ in all systems whereby the increase of tan δ is more pronounced. There are no significant changes in the dielectric properties by adding the polymeric flame retardants, which can be attributed to the chemical similarity of PBT and PET-P. In contrast to these polymeric systems, low-molar mass flame retardants diminish the dielectric properties in a stronger way[29] because of a higher dielectric constant of the additives especially at high loadings necessary for halogen-free flame retardancy. Therefore, the presented polymeric compounds can be used in typical applications without any loss of insulating properties.

Mechanical Performance

The mechanical properties are often very strongly affected by adding flame retardants. As reported in a previous study,[7] the incorporation of low-molar mass substances like aluminum phosphinates embrittle the tough PBT matrix. Therefore, chemistry strikes out in new directions by developing polymeric flame retardants to reduce the effect on mechanical properties.

The tensile and impact results of the new polymeric flame-retarded PBT compounds are presented in Table V.

The comparison of the base polymer PET-P-DOPO to PBT shows that PET-P-DOPO has generally considerably lower mechanical properties. Tensile strength σ_m, elongation at break ε_b, and impact strength a_{cu} decrease by more than 80% and reflect especially a very brittle response. Only the Young's modulus E is higher than that of PBT. The other PET-P polymers were not mechanically characterized, because injection molding of the brittle materials was not possible, but it is expected that PET-P-DPPO and PET-P-DPhPO will show comparable values because of their chemical comparability.

By adding the PET-P polymers to PBT, the Young's modulus raised in all blend systems. This can be justified on the one hand by a higher modulus of the PET-P polymers in comparison to PBT. On the other hand, the normalized crystallinity referred to the PBT matrix is enhanced by at least 10% in all blend systems. Therefore, according to Tsai-Halpin,[30] the increase of Young's modulus also results from enhanced crystallinity (see Table I).

The tensile strength of the immiscible blends is reduced slightly because of a relatively low strength of the polymer PET-P and weak phase adhesion. However, the decrease of tensile strength

Table V. Mechanical Properties of PBT, PET-P-DOPO, and the Blend Systems Obtained by Static Tensile Tests and Unnotched Charpy Tests at Room Temperature: Young's Modulus E, Tensile Strength σ_m, Elongation at Break ε_b, and Impact Strength a_{cu}

Material	E (MPa)	σ_m (MPa)	ε_b (%)	a_{cu} (kJ/m^2)
PBT	2170 ± 30	54 ± 1	17 ± 6	190 ± 4
PET-P-DOPO	2570 ± 90	10 ± 2	0.35 ± 0.1	0.6 ± 0.1
PBT/PET-P-DOPO	2320 ± 60	52 ± 1	3 ± 0.5	21 ± 2
PBT/PET-P-DPPO	2510 ± 20	49 ± 1	2 ± 0.5	17 ± 2
PBT/PET-P-DPhPO	2670 ± 40	50 ± 1	2 ± 0.5	19 ± 2

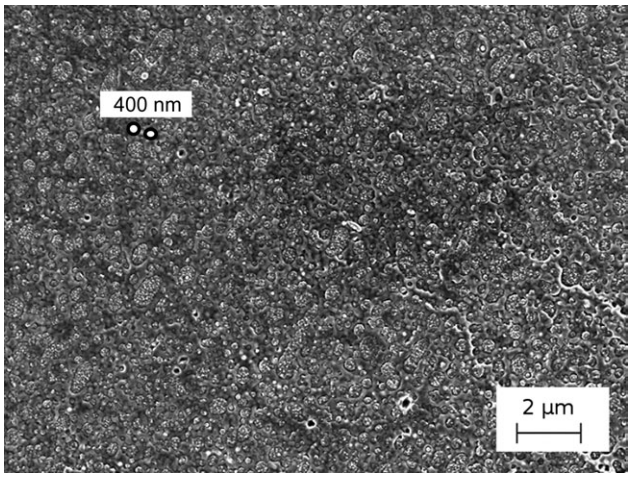

Figure 10. SEM picture of fracture surface after impact testing of the compatibilized blend PBT/PET-P-DOPO/PBT-*co*-PET-P-DOPO. Magnification: 5000×. Two droplets are exemplary highlighted with the average droplet size of 400 nm.

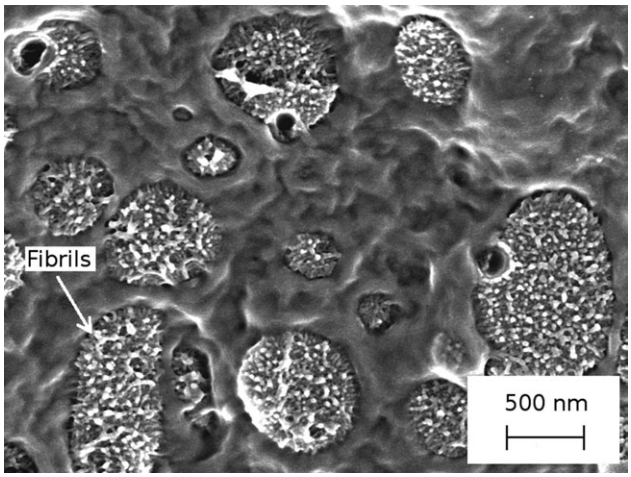

Figure 11. SEM picture of fracture surface after impact testing of the compatibilized blend PBT/PET-P-DOPO/PBT-*co*-PET-P-DOPO. Magnification: 20,000×.

in the blends is not significant. The main difference between PBT and the flame-retarded blends is the elongation at break and impact strength, which is strongly reduced by more than 90%. This behavior can be explained by the brittle behavior of the PET-P polymers. The immiscibility and the weak phase adhesion of the amorphous PET-P to the semicrystalline PBT also contribute to the decrease of impact strength.

The problem of embrittlement also exists in the use of low molar mass flame retardants for PBT.[9] Comparing PBT mixtures with commercial flame retardants based on aluminum phosphinates at comparable additive concentrations, the impact strength is strongly affected in the same magnitude. On the other hand, the tensile strength of those compounds is significantly reduced, whereas the blends studied here showed a better tensile behavior. The differences arise from different stress transfer mechanisms. In the blend systems with polymeric flame retardants, the stress can be transferred into the matrix and also into the second phase. In contrast, the low molar mass flame retardants exist as stiff particles within the PBT matrix, and no stress can be introduced. They act as imperfections which in turn result in a lower tensile strength.[9]

In this respect, the different phase morphology of the blends has no significant influence on the mechanical properties. The blends show a similar mechanical behavior with only slight differences that cannot be assigned to differences in structure.

The low impact strength of the blends is generally not acceptable for given applications and has thus to be improved. Possible solutions that appear include changing the chemical structure of the phosphorus polyesters, adding an impact modifier, or optimizing the phase adhesion. Some of the concepts will be discussed in the next part.

Improvement of Miscibility and Impact Properties

In this chapter, an approach is introduced to improve the impact strength by enhancement of the phase adhesion between PBT and the polymeric PET-P-DOPO. A copolymer of PBT and PET-P-DOPO named PBT-*co*-PET-P-DOPO may act as compatibilizer between the phases to improve the phase adhesion. By compatibilization of the phases, an improved impact strength may be expected.

The copolymer is added at a concentration of 5 wt % to the blend PBT/PET-P-DOPO. Investigating the morphology by SEM (Figure 10) reveals indeed a refined phase morphology in comparison to the noncompatibilized blend (Figure 10). The phase separated morphology is still observed after adding the copolymer, but the mean phase size decreases from 1 µm to 400 nm. A compatibilization effect is assumed, because there are additionally fibrils between the PBT matrix and the second phase, which is shown at 20,000× magnification in Figure 11. Assuming more interactions between the phases by generation of a pancake interfacial structure the interfacial tension mutually decreases and leads to a higher capillary number and therefore to a smaller droplet phase size. Additionally, only two phases instead of three are visible. Modulated DSC measurements of the glass transition also reveal two T_gs (Table VI).

The T_g at 60°C reflects the glass transition of the base polymer PBT. The second T_g can be allocated neither to the base polymer PET-P-DOPO nor to the copolymer PBT-*co*-PET-P-DOPO. The state of mixing can be calculated by means of the Fox equation[31] relating the weight fractions of the components to

Table VI. Glass Transition Temperatures of the Blend System PBT/PET-P-DOPO with and without Compatibilizer Obtained by Modulated DSC from the Reversing Heat Flow Signal

Material	T_{g1} (°C; ±1)	T_{g2} (°C; ±1)	T_{g3} (°C; ±1)
PBT/PET-P-DOPO	60	144	-
PBT-*co*-PET-P-DOPO	-	-	117
PBT/PET-P-DOPO/ PBT-*co*-PET-P-DOPO	60	139	-

Table VII. Flammability (Reaction to a Small Flame) of PBT and the Investigated Blends of PBT with Phosphorus Polyesters in LOI (error ± 1.0%) and UL 94

Material	LOI (%)	UL 94
PBT	21.8	V-2
PBT/PET-P-DOPO	22.4	HB
PBT/PET-P-DPPO	21.1	HB
PBT/PET-P-DPhPO	22.5	V-2
PBT/PET-P-DOPO/PBT-*co*-PET-P-DOPO	21.5	HB

the glass transition temperature. The calculated T_g value for miscibility of PBT-*co*-PET-P-DOPO in PBT is 63°C, in PET-P-DOPO it is 140°C. The T_g of the blend measured at 139°C fits within the error to the calculated T_g of 140°C suggesting miscibility of PBT-*co*-PET-P-DOPO in PET-P-DOPO. Also there is no change in glass transition temperature of the PBT phase the formed fibrils reflects the partial compatibility between the PBT phase and the miscible PET-P-DOPO/PBT-*co*-PET-P-DOPO phase.

The smaller phase size in the compatibilized blend and the improved phase adhesion lead to an enhancement of impact properties. Incorporation of the amorphous bulky PET-P-DOPO polymer caused a 90% drop of Charpy impact strength from 190 to 21 kJ/m^2. Adding the compatibilizer yields an improvement of 25% in impact strength to 29 kJ/m^2 compared the not compatibilized blend.

Therefore, this compatibilizing approach is promising and can be considered as a correct step into the direction of enhancing the mechanical properties deteriorated by the addition of polymer flame retardants. It will be pursued in the future by further variations in the chemical structure of the copolyesters.

Flammability and Burning Behavior

PBT is flammable as is evidenced by the LOI value of 21.8% and the V-2 classification in the UL 94 (Table VII). A UL 94 HB classification "(horizontal burning)" was often reported for PBT instead of V-2. The difference in the UL 94 behavior between a HB and a V-2 material is very small in this case. PBT and all of its investigated blends showed extensive flaming dripping. In the case of PBT and PBT/PET-P-DPhPO, the dripping led to extinguishment of the sample yielding V-2. Concerning the HB materials, the dripping did not lead to extinguishment. PBT and its investigated blends showed very similar behavior not only in UL 94 but also in LOI. The addition of the phosphorus polyesters did not lead to a significant increase in LOI. This does not mean that there is no flame retardancy effect, because LOI does generally correlate neither with other fire tests nor with a material's behavior in a real fire.[32]

Fire tests under forced-flaming conditions in the cone calorimeter revealed differences in the burning behavior (Table VIII). All of the investigated blends showed a similar reduction in total heat evolved (THE). A reduction in peak heat release rate (pHRR) that was similar for PBT/PET-P-DPPO, PBT/PET-P-DPhPO, and PBT/PET-P-DOPO/PBT-*co*-PET-P-DOPO and strongest for PBT/PET-P-DOPO, was found as well. This proves a flame retardancy effect of the phosphorus polyesters in PBT. The addition of the phosphorus polyesters to PBT increased the residue from 3 wt % (PBT) to 8–10 wt %. Thus, a condensed-phase mechanism was active in the blends of PBT with the phosphorus polyesters. Furthermore, flame inhibition was evidenced by the decrease in effective heat of combustion (THE/TML, TML = total mass loss). The gas-phase activity of the investigated blends of PBT with phosphorus polyesters was equally strong, because the reduction in THE/TML was very similar. Thus, two flame-retardancy mechanisms, that is, flame inhibition and condensed-phase activity, were simultaneously active in the investigated blends of PBT with phosphorus polyesters.

CONCLUSIONS

Improving halogen-free flame retardancy using polymeric additives is very promising, because the chemically bound additives can be dispersed in the polymer matrix and a lower influence on the material's properties can be expected.

In this work, three new polymers, based on phosphorus polyesters, were introduced to be used as flame retardants for PBT. The addition of phosphorus polyesters leads to the formation of immiscible blend systems. A lower viscosity ratio causes a more continuous droplet phase. Addition of a copolymer based on the two base polymers leads to a compatibilizing effect as shown by smaller phases and better phase adhesion.

Under the very specific conditions of LOI and UL 94, PBT and its blends with phosphorus polyesters showed similar results. Clear flame-retardancy effects were proved by cone calorimetry. The pHRR and THE of the blends were reduced and the residue increased compared to PBT. Flame inhibition and condensed-

Table VIII. Results Obtained by Cone Calorimetry with an External Heat Flux of 50 kW/m^2

Material	pHRR (kW/m^2)	THE (MJ/m^2)	Residue (wt %)	THE/TML (MJ/m^2 g)
PBT	1713 ± 100	72 ± 2	3 ± 1	2.2 ± 0.1
PBT/PET-P-DOPO	1091 ± 40	55 ± 2	10 ± 2	1.7 ± 0.1
PBT/PET-P-DPPO	1212 ± 60	56 ± 2	9 ± 1	1.8 ± 0.1
PBT/PET-P-DPhPO	1347 ± 70	54 ± 2	8 ± 2	1.7 ± 0.1
PBT/PET-P-DOPO/PBT-*co*-PET-P-DOPO	1317 ± 180	59 ± 2	10 ± 4	1.9 ± 0.1

Errors based on maximum deviation of average values.

phase activity were evidenced as flame-retardancy mechanisms that are simultaneously active in the blends of PBT with phosphorus polyesters.

For the wide applications range of PBT, not only the flame retardancy but also the dielectric and mechanical behaviors play a major role. No significant influence on the dielectric properties due to the addition of the polymer flame retardants was observed. In contrast, the addition of the bulky amorphous PET-P polymers leads to an embrittlement of the matrix, whereas the tensile strength is not affected. The deterioration of impact strength is similar to low-molecular weight additives like metal phosphinates. A promising approach to improve the impact strength is adding a copolymer whereby the impact strength could be improved by 25%. Future investigations will be aimed in this direction to achieve a higher toughness of flame-retarded PBT, which is currently a major problem when using flame-retarded polymers.

ACKNOWLEDGMENTS

The financial support of the German Research Foundation (DFG) in the frame of the research project numbers Al 474 17-1, DO 453/7-1, Po 575/11-1, and Scha 730/11-1 is highly acknowledged. PBT was kindly provided by BASF SE. The authors further acknowledge Florian Stegmann, Anne Lang, and Ute Kuhn (Department of Polymer Engineering) for the experimental support.

REFERENCES

1. EU-Council and Parliament. RoHS–Directive, 2002/95/EC, **2003**.
2. EU-Council and Parliament. WEEE–Directive, 2002/96/EC, **2003**.
3. Levchik, S. V.; Weil, E. D. *Polym. Int.* **2005**, *54*, 11.
4. Gallo, E.; Schartel, B.; Braun, U.; Russo, P.; Acierno, D. *Polym. Adv. Technol.* **2011**, *22*, 2382.
5. Braun, U.; Bahr, H.; Sturm, H.; Schartel, B. *Polym. Adv. Technol.* **2008**, *19*, 680.
6. Brehme, S.; Schartel, B.; Goebbels, J.; Fischer, O.; Pospiech, D.; Bykov, Y.; Döring, M. *Polym. Degrad. Stab.* **2011**, *96*, 875.
7. Köppl, T.; Brehme, S.; Wolff-Fabris, F.; Altstädt, V.; Schartel, B.; Döring, M. *J. Appl. Polym. Sci.* **2012**, *124*, 9.
8. Braun, U.; Schartel, B. *Macromol. Mater. Eng.* **2008**, *293*, 206.
9. Wang, C. S.; Lin, C. H.; Chen, C. Y. *J. Polym. Sci. Part A: Polym. Chem.* **1988**, *36*, 3051.
10. Pospiech, D.; Jehnichen, D.; Komber, H.; Korwitz, A.; Janke, A.; Hoffmann, T.; Kretzschmar, B.; Häußler, L.; Reuter, U.; Döring, M.; Seibold, S.; Perez-Graterol, R.; Sandler, J. K. W.; Altstädt, V.; Bellucci, F.; Camino G. *Nanostruct. Polym. Nanocompos.* **2008**, *4*, 62.
11. Fischer, O.; Pospiech, D.; Korwitz, A.; Sahre, K.; Häußler, L.; Friedel, P.; Fischer, D.; Bykov, Y.; Döring, M. *Polym. Degrad. Stab.* **2011**, *96*, 2198.
12. Sablong, R.; Duchateau, R.; Koning, C. E.; Pospiech, D.; Korwitz, A.; Komber, H., Starke, S.; Häußler, L.; Jehnichen, D.; Auf der Landwehr, M. *Polym. Degrad. Stab.* **2011**, *96*, 334.
13. Pospiech, D.; Häußler, L.; Korwitz, A.; Fischer, O.; Starke, S.; Jehnichen, D.; Köppl, T., Altstädt, V. *High Perform. Polym.* **2012**, *24*, 64.
14. Brehme, S.; Köppl, T.; Schartel, B.; Fischer, O.; Altstädt, V.; Pospiech, D.; Döring, M. *Macromol. Chem. Phys.*, to appear, DOI: 10.1002/macp.201200072.
15. Wunderlich, B. Thermal Analysis of Polymeric Materials; Springer: Berlin, **2005**.
16. Grand, A. F.; Wilkie, C. A. Fire Retardancy of Polymeric Materials; Marcel Dekker: New York, **2000**; pp 285–352.
17. Sonnier, R.; Viretto, A.; Taguet, A.; Lopez-Cuesta, J.-M. *J. Appl. Polym. Sci.* **2012**, *125*, 3148.
18. Basch, A.; Lewin, M. *J. Polym. Sci. Part A: Polym. Chem.* **1973**, *11*, 3071.
19. Basch, A.; Lewin, M. *J. Polym. Sci. Part A: Polym. Chem.* **1973**, *11*, 3095.
20. Robeson, L. M. Polymer Blends: A Comprehensive Review; Hanser: Munich, **2007**.
21. Creton, C.; Kramer, E. J.; Brown, H. R.; Hui, C. -J. *Adv. Polym. Sci.* **2002**, *156*, 53.
22. Taylor G. I. *Proc. R. Soc. Lond. A* **1932**, *138*, 48.
23. Grace, H. P. *Chem. Eng. Commun.* **1982**, *14*, 225.
24. Utracki, L. A. *J. Rheol.* **1991**, *35*, 1615.
25. Majumdar, B.; Paul, D. R.; Oshinski, A. *J. Polymer* **1997**, *38*, 1787.
26. Puyvelde, P. V.; Velankar, S.; Moldenaers, P. *Curr. Opin. Colloid Interface Sci.* **2001**, *6*, 457.
27. Tucker, C. L.; Moldenaers, P. *Annu. Rev. Fluid Mech.* **2002**, *34*, 177.
28. Graebling, D.; Muller, R.; Palierne, J. F. *Macromolecules* **1993**, *26*, 320.
29. Kim, D. K.; Park, S. D.; Yoo, M. J.; Lee, W. S.; Kang, N. K.; Lim, J. K.; Kyoung, J. B. *Polymer (Korea)* **2009**, *33*, 39.
30. Halpin, J. C.; Kardos, J. L. *Polym. Eng. Sci.* **1976**, *16*, 344.
31. Fox, T. G. *Bull. Am. Phys. Soc.* **1956**, *1*, 123.
32. Weil, E. D.; Patel, N. G.; Said, M. M.; Hirschler, M. M.; Shakir, S. *Fire Materials* **1992**, *16*, 159.